Effect of Window Size on PIV

A Parametric Study

Bilal Abdul Halim

Abstract

When there exists a high enough potential drop between two electrodes, a *corona discharge* is created, carrying high velocity ions. Through the exchange of their kinetic energies, these ions drive whatever fluid or medium between. Here, silicone oil of dynamic viscosity 50 cst is driven in a channel through the aforementioned *corona discharge*. In this study Particle Image Velocimetry *(PIV)* is done to study the flow of the oil. In addition to that, a parametric study is performed on varying the interrogation window sizes to see it's effect on PIV accuracy.

Experimental Fluid Mechanics (MIME6450)

Dr. Choueiri

List of Symbols

The next list describes several symbols that will be later used within the body of the document

δ_z	Depth of field
λ	Wave length of incident light
μ_f	Fluid dynamic viscosity
$\phi_{II'}(x, y)$	Cross correlation map
ρ_p	Particle density
τ_f	Fluid characteristic time
τ_p	Particle characteristic time
C_c	Cunningham coefficient
d_p	Particle diameter
d_{diff}	Smallest diameter imaged
$f_\#$	F number (ratio of lens focal length to lens aperture)
I, I'	Intensity distributions in first and second frame, respectively
i, j	Interrogation window position
L_c	Characteristic length
M	Magnification factor
St	Stokes number
U_c	Characteristic velocity
x, y	Spacial shift
Z_0	Distance between object plane and lens
z_0	Distance between image plane and lens

1 Introduction

Evaluating the velocity of a homogeneous fluid directly through an optical device is not feasible. This is where Particle Image Velocimetry, or *PIV* comes in handy. By adding tracers into the fluid and shining an almost two-dimensional laser sheet, the flow velocity can be resolved; this can be done by imaging those tracers at two different, but simultaneous, instances. PIV has it's advantages, as it provides higher spacial resolution as compared to something like LDV or Hot wire. Having said that, LDV and Hot wire are still used and provide better temporal resolution. When it comes to designing and building a PIV setup, the experimentalist has to be aware of all the nuances that go into the setup, as the simplest mistake can lead to unreliable and inaccurate data. There are also compromises to be made.

In this paper, I discuss the background and theory behind particle image velocimetry. I will also be conducting a parametric study on the interrogation window size, to see it's effect in terms of accuracy.

2 Background & Theory

2.1 Typical Setup

Usually, a typical PIV setup has to include a laser with which a laser sheet is created. This aims to only illuminate the cross-sectional area of interest in the fluid medium, as seen in figure 1. From there, one can image those illuminated particles at two consecutive time instances. By computing how far the particles traveled from one frame to the next, the velocity field can be resolved.

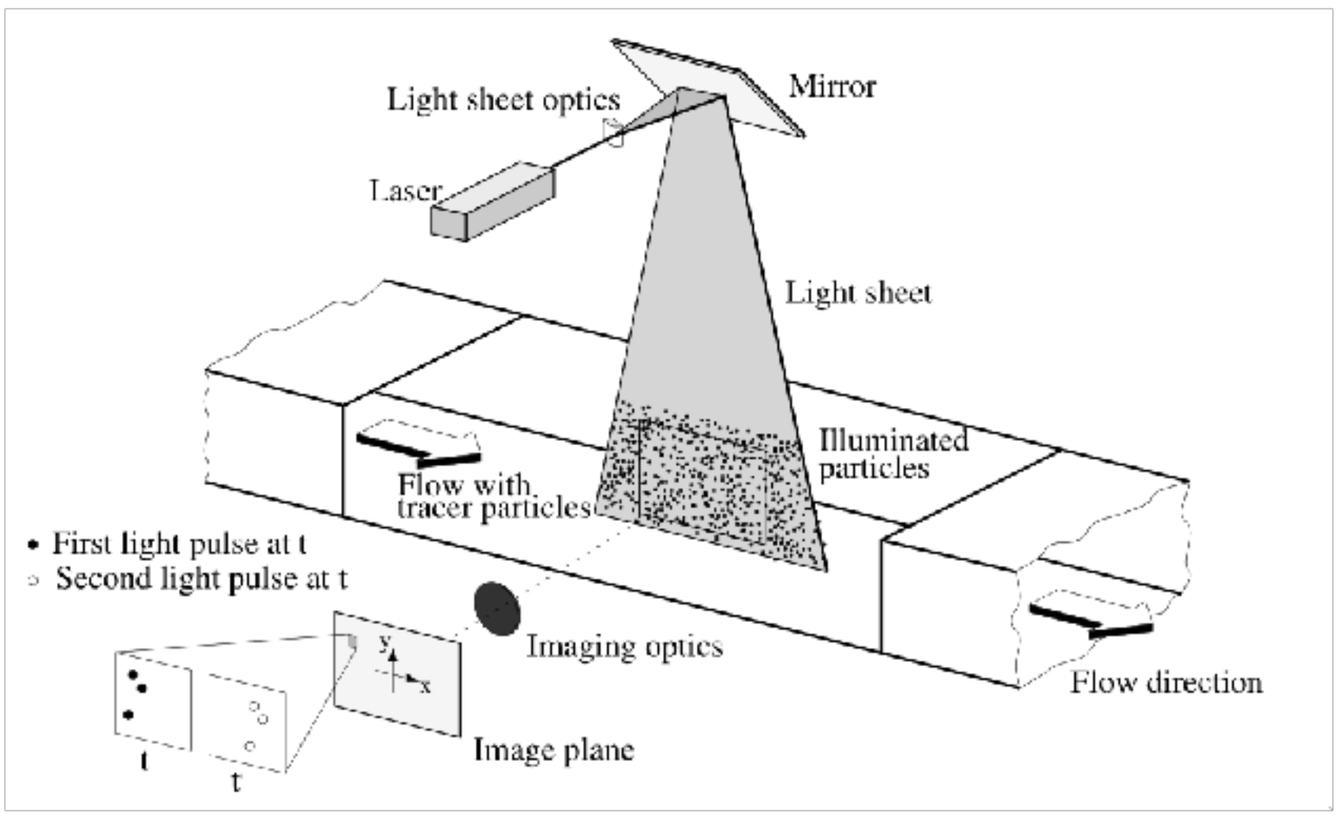

Figure 1: Experimental arrangement for PIV in a wind tunnel

Type	Material	Mean diameter in μm
Solid	Polystyrene	10 - 100
	Aluminum	2 - 7
	Glass spheres	10 - 100
	Granules for synthetic coatings	10 - 500
Liquid	Different oils	50 - 500
Gaseous	Oxygen bubbles	50 - 1000

Table 1: Seeding material for liquid flows

2.2 Tracers

Tracers are undoubtedly one of the most important components of the PIV setup, as one needs to choose the tracers in a way where they follow the flow as faithfully as possible. The first compromise to be made is picking particles that are small enough to follow the flow, yet large enough to scatter enough light for imaging purposes. The experimentalist can calculate a widely recognized number as an indicator for the traceability of particles, and that is the Stokes number St

$$St = \frac{\tau_p}{\tau_f} = \frac{\tau_p U_c}{L_c} = \frac{\rho_p d_p^2 U_c Cc}{18\mu_f L}, \tag{1}$$

where This number expresses the ratio of the characteristic time of the particle

$$\tau_p = \frac{\rho_p d_p^2}{18\mu_f}$$

to the characteristic time of the fluid itself.

$$\tau_f = \frac{L_c}{U_c}$$

Although purchased tracers will almost always follow the flow the flow as faithfully as possible, it is always good to calculate the Stokes number, which has to satisfy the following condition.

$$St << 1.$$

For a more in depth analysis on choosing the correct tracers, please read [1]. Table 1 shows the typical tracers used in liquid flow PIV [2].

2.3 Imaging and Preprocessing

Imaging tracers can be a little challenging if one does not have the correct lens or has not tweaked the camera settings to the correct ones. Firstly, the reason one sees the tracers is because of the scattering of the laser sheet. The more tracers in the fluid, the more the scattering and the higher the image intensity

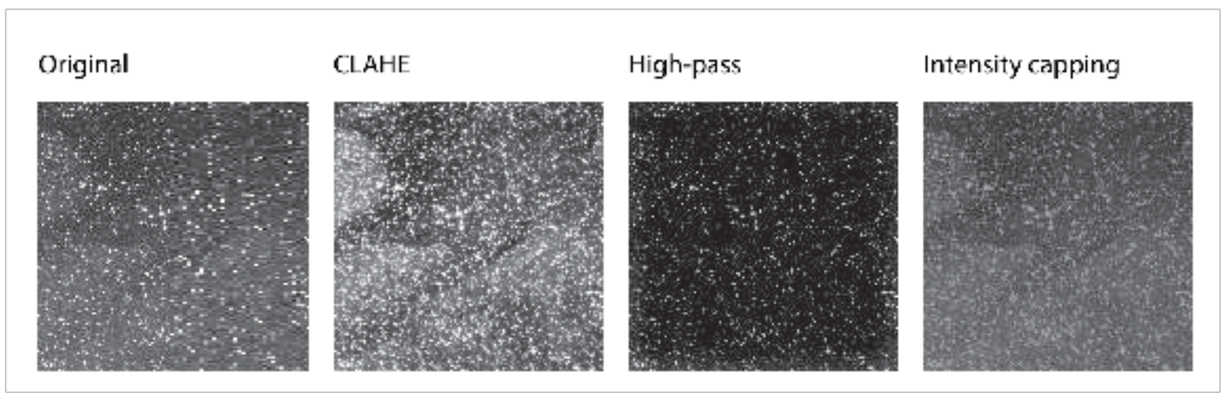

Figure 2: Effect of several preprocessing filters

(brighter image), which can be an economical solution if changing laser intensity is not feasible. In order to obtain a sharp image with all illuminated particles in focus, the camera depth of field δ_z has to be calculated and bigger than the laser sheet thickness t. According to [2], depth of field is given as

$$\delta_z = 2f_{\#}d_{diff}\frac{M+1}{M^2}. \tag{2}$$

To be able to calculate that depth of field, the f number $f_{\#}$ can be adjusted, depending if the lens has an adjustable aperture ring, and the magnification factor M can be calculated as the ratio of the distance between the image plane and lens z_0 to the distance between the object plane and lens Z_0.

$$M = \frac{z_0}{Z_0}.$$

Lastly, the smallest diameter to be imaged by the lens d_{diff} can be found as

$$d_{diff} = 2.44f_{\#}(M+1)\lambda.$$

Now that the images are captured, some preprocessing needs to be performed to filter out any unwanted intensities. This goes without saying, but it is much more advisable to build the setup in a way were the experimentalist is blocking out as much unwanted light as possible, but sometimes, even with the best setups, we still get unwanted reflections from light scattered by the tracers themselves. One filter that can and should always be applied is the intensity capping filter. This filter looks at spots with a high intensity, much higher than the mean intensity of the image. Those bright spots are then reduced accordingly. This filter aims to enhance the cross correlation peak (which will be discussed later on), and reduce the bias from bright spots [3]. Figure 2 shows some of the filters that can be applied and their affect on the image [4]. Another important filter to apply is the high-pass filter, which as the name implies, filters out intensities above a certain thresholds, and zeros everything below. This filter aims to accentuate the tracers and make them much more prevalent in the image.

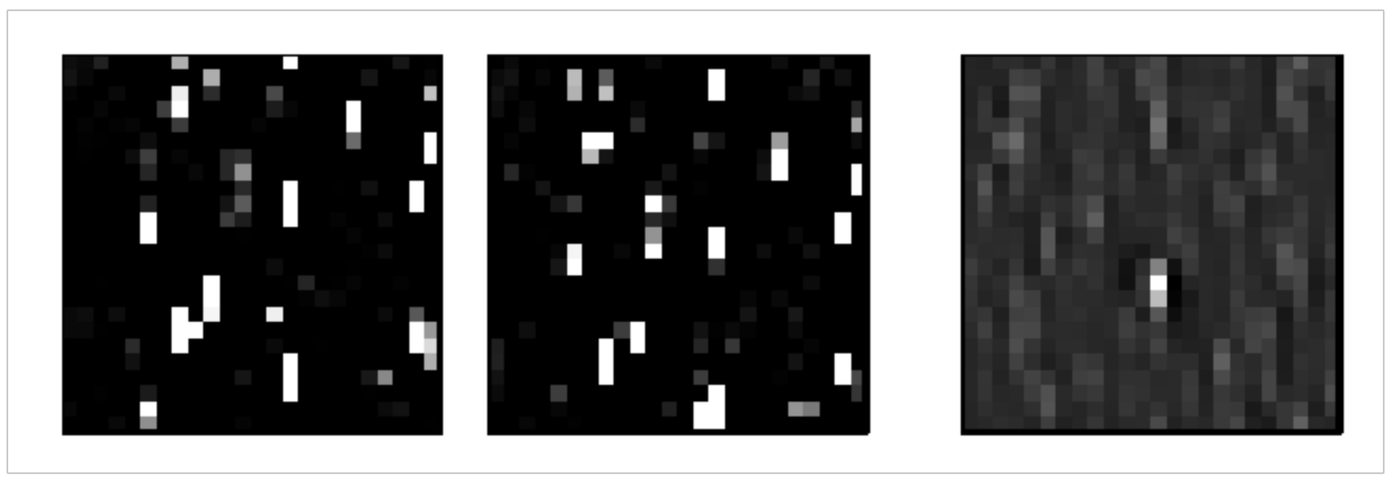

Figure 3: Interrogation window at two instances and its corresponding correlation intensity

2.4 Cross-Correlation

It is important to note here that this study focuses on the effect of interrogation window size (explained later) on PIV, and not PTV (Particle Tracking Velocimetry). We are not tracking individual particles, instead dividing the image into square sub domains in a way were all particles within that sub domain/interrogation window are assumed to have a uniform velocity. To be able to resolve the velocity field across the entire area of interest, we can study the Grey intensity distribution of those sub domains at two different frames (by considering a square matrix of intensity values). By multiplying and adding those intensity distributions, this will give another matrix with the same size but with one prevalent intensity value. By measuring the distance from the centroid to that intensity value, we have the most probable movement of the particles within that interrogation window. What I said is a mouthful which can be summed up below

$$\phi_{II'}(x,y) = \sum_{i=-\infty}^{\infty} \sum_{j=-\infty}^{\infty} [I(i,j)][I'(i+x,j+y)]. \tag{3}$$

The cross correlation function $\phi_{II'}(x,y)$ can be computed using either the method I explained above, which solves the cross correlation function in the spacial domain, known as DCC (Direct Cross Correlation), or by computing the cross correlation function in the frequency domain.

Another way to look equation 3 can be found in figure **??**, where the first two images correspond to the distribution of tracers within the same interrogation window at two instances in time. So we can represent the intensity distribution of the first image as I and that of the second image as I'. Multiplying and adding those two images based on equation 3 gives us the third image, which represents the cross correlation function $\phi_{II'}(x,y)$. A discernible bright spot can be seen, which represents the most probable displacement of all particles within that interrogation window.

3 Technique

The setup I am working with is designed to drive/pump the fluid medium in an open curved channel. This works by creating a potential drop and introducing a high input voltage which creates a discharge known as the Corona Discharge. The bigger picture of the project is to find an optimum way of creating stable water emulsions in oil. But as far as this paper goes, I am strictly looking at the flow itself. The schematic of the setup is shown in figure 4. The discharge created from the needle and the copper ground electrode is what's creating the flow in silicone oil. The channel in which the fluid flows is made of a two glass petri dishes, with the smaller one placed upside down in the center of the bigger one (to create a channel). On the opposite end sits a laser with a cylindrical lens parallel to the ground. Because I could not mount the highs-peed camera in a way where it is imaging vertically downwards, I had to place a 45 degree mirror right above the laser sheet. This way the camera is imaging vertically downwards at the flow, which is what I needed. The needle is connected to a signal generator which is connected to a power source, able to output up to 10kV of voltage.

3.1 Equipment

- Green laser
- High-speed camera (Oylmpus TR i-Speed)
- Mirror (Amazon Basic 3-inch circular mirror)
- Petri dish
- Signal Generator/Multimeter (Keithley 2100)
- Power source (BK 1698)
- Amplifier ($\pm$ 10 kV TREK Model 10/10B)
- Copper strip (Copper tape)
- Tracers (10 μm glass spheres)
- Cylindrical lens (Edmund Optics)
- Silicone Oil 50cst (from MicroLubrol)
- Needle electrode (superfine tungsten needle)
- Steel breadboard (Edmund Optics)

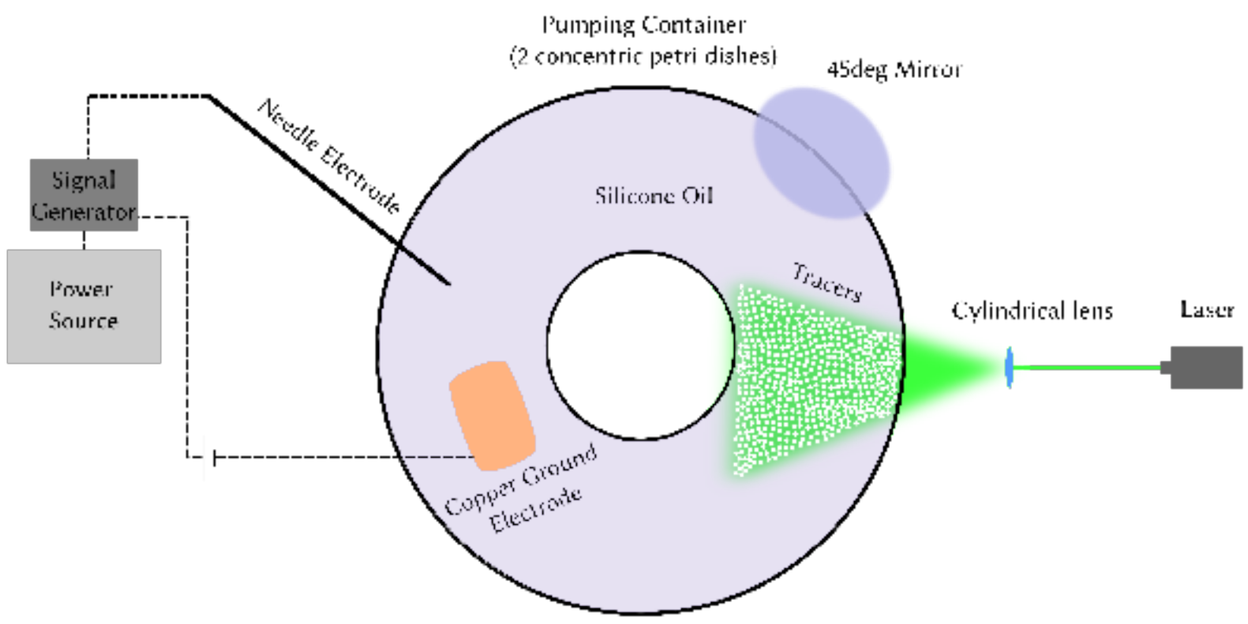

Figure 4: Schematic of the setup

4 Discussion

Silicone oil of 50 cst kinematic viscosity (purchased from MicroLubrol) was used as the fluid liquid, and through momentum transfer of the ionic wind coming from the corona discharge, silicone oil circulates in the pumping apparatus (figure 4). The hollow glass spheres with diameter of 10 μm where mixed in a sonication water bath with the oil for 10 minutes prior to testing, to guarantee as much dispersion and uniformity of tracers within the fluid as possible. And by examining one of the frames taken in figure 5, one can agree the tracers are distributed fairly uniformly. After shining the laser sheet onto the surface of the oil, the oil was imaged for 2.66 seconds at 30 fps, thus generating 80 frames, all of which were processed.

A parametric study of varying window sizes was done to study the accuracy of that perimeter on the data. A total of 6 configurations were conducted. Two window sizes (32 and 24 pixels) were used as one pass, meaning the cross correlation function $\phi_{II'}(x, y)$ is only solved once. The four remaining window size configurations were multiple passes. With such configuration, the cross correlation function $\phi_{II'}(x, y)$ is solved multiple times, depending on the number of passes (windows concatenated). Figure 6 shows the difference in sizes of each configuration used.

For my PIV analysis, I used *PIVlab*, which is a program written in MATLAB. Through *PIVlab* I was able to run my PIV on 80 consecutive frames, and the results that will proceed are the temporal average of all 80 frames, as the flow is laminar. After obtaining x, y, u, v data from the program, I was able to generate velocity contour plots for every configuration.

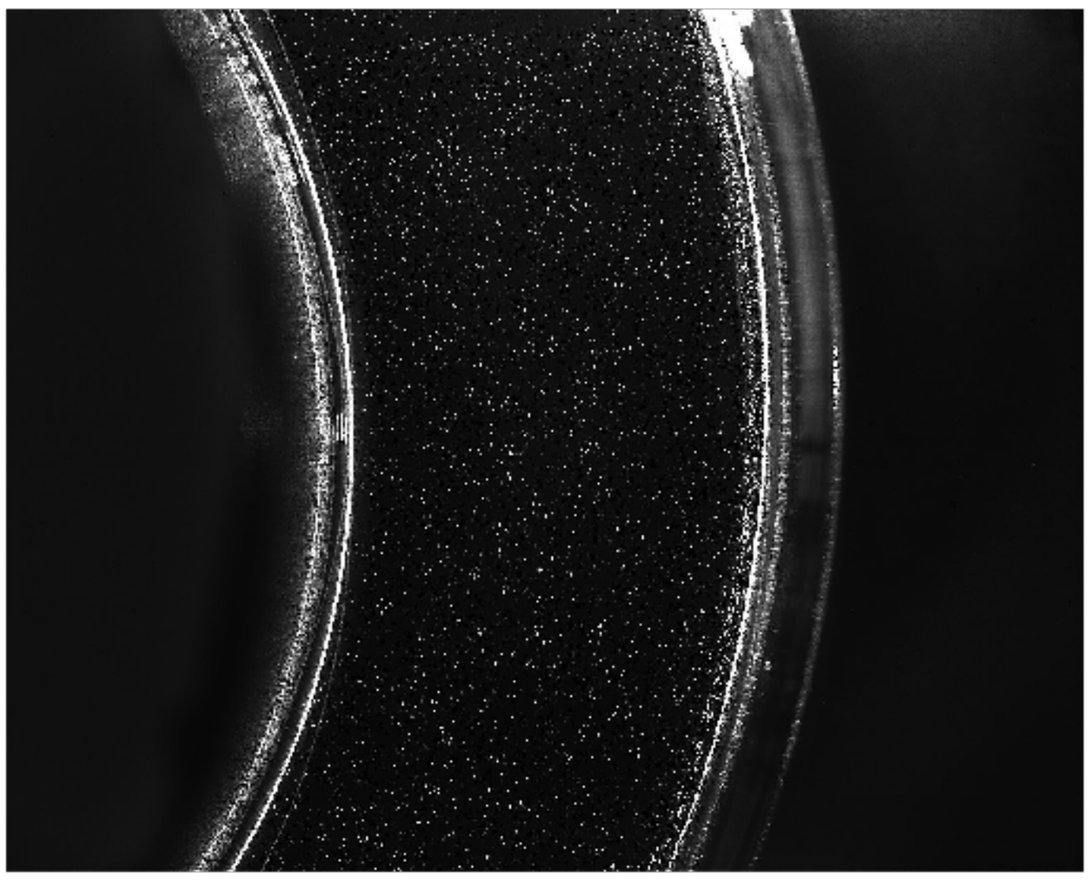

Figure 5: Photo of tracers in Silicone oil

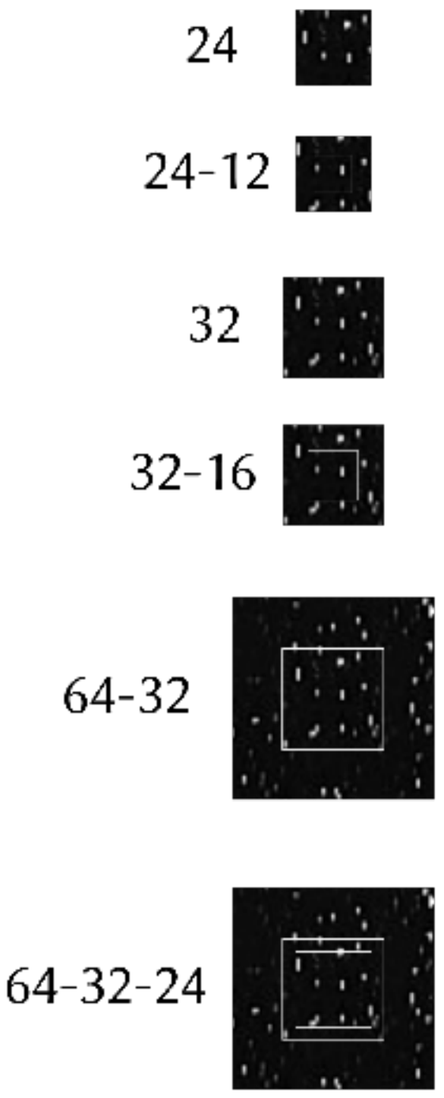

Figure 6: Different interrogation window configurations used

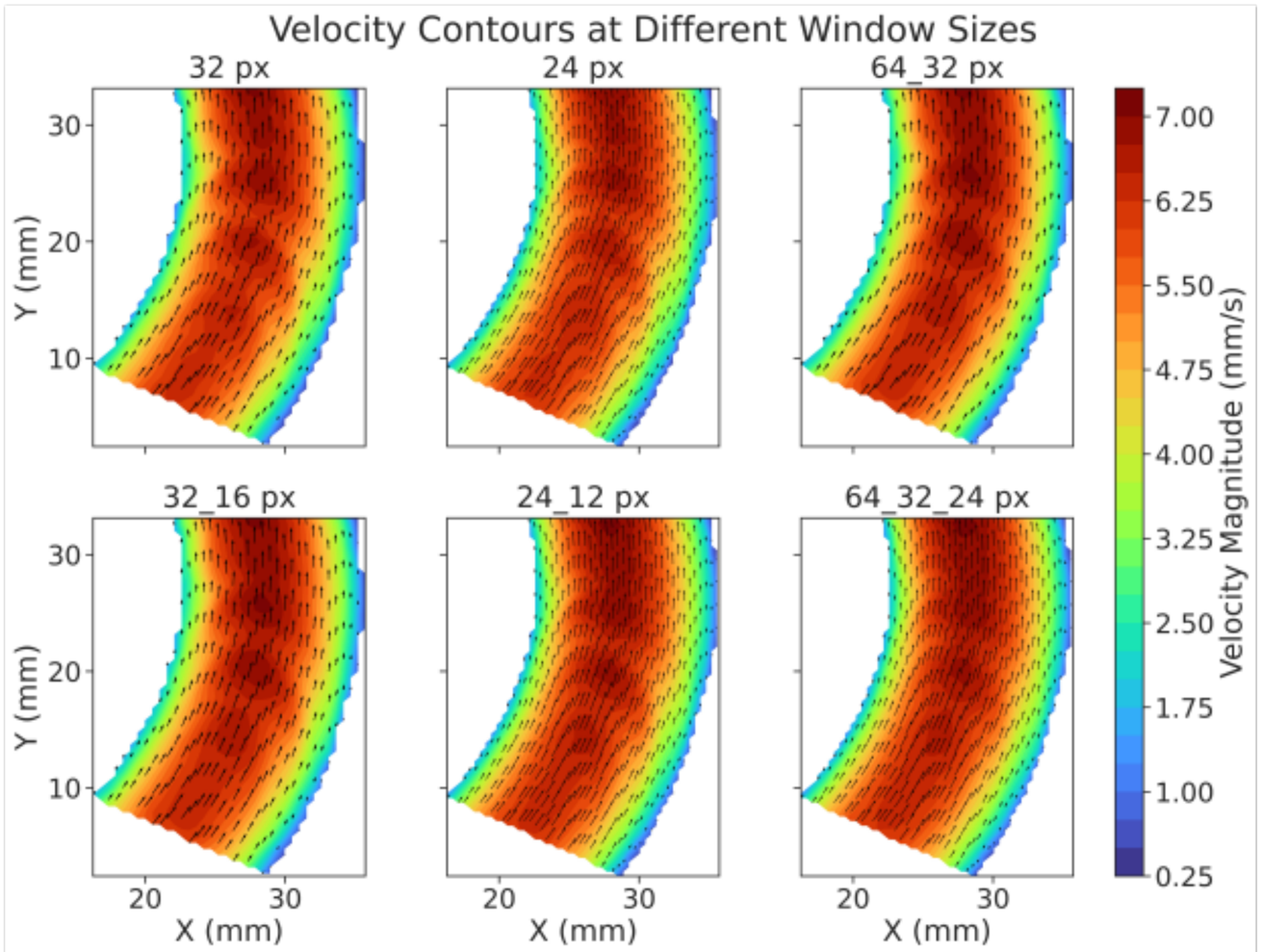

Figure 7: Velocity contours at different window sizes

It is hard to tell the effect of the different window size configuration from this plot, but when using a multip-pass configuration, there is a much smoother gradient (i.e a more defined transition) between velocity values. Another thing to point out is with decreasing the window size, a lot more particles' velocity is being computed, which in turn increases the density of the arrows (quiver plot layed on top of the contour plot in figure 7). Here I scaled the density of the arrows by 5 as it will be difficult to see the contour plot itself. The velocity values can also be looked at differently, as a distribution instead of contour plot. By examining figure 8, we can see that the larger window sizes do not contain as much velocity data, while with multip pass configuration, such as 64-32-24 pixel window configuration, there are sufficient data points for the entire range of velocities.

I also plotted the velocity magnitude profile accross the channel width for all configurations (figure 9).

From figure 9, it can be seen that the 24 pixel window size as well as the 24-12 multi-pass configuration had noticeably jagged velocity profiles. This can be attributed to the fact that not only were there insufficient tracers within that window size, but also because the tracers tend to escape the window between two instances. The pixel and 32-16 pixel window configuration showed a marginal improvement, but with relatively sharp edges as well. Lastly, the 64-32 and 64-32-24 pixel window configuration showed the best and smoothes profiles out of all the other configuration. This is because this configuration not only accounted

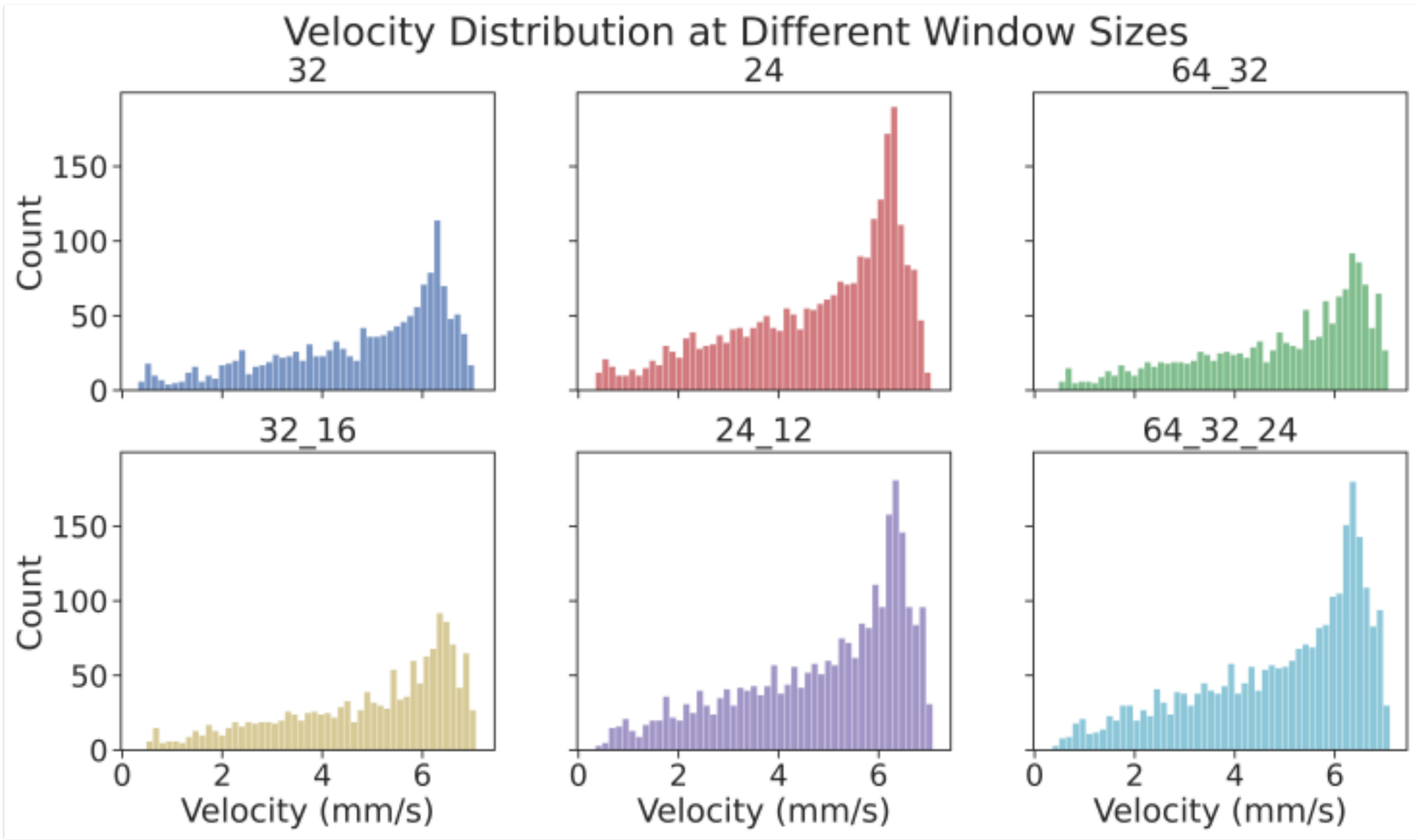

Figure 8: Velocity distribution at different window sizes

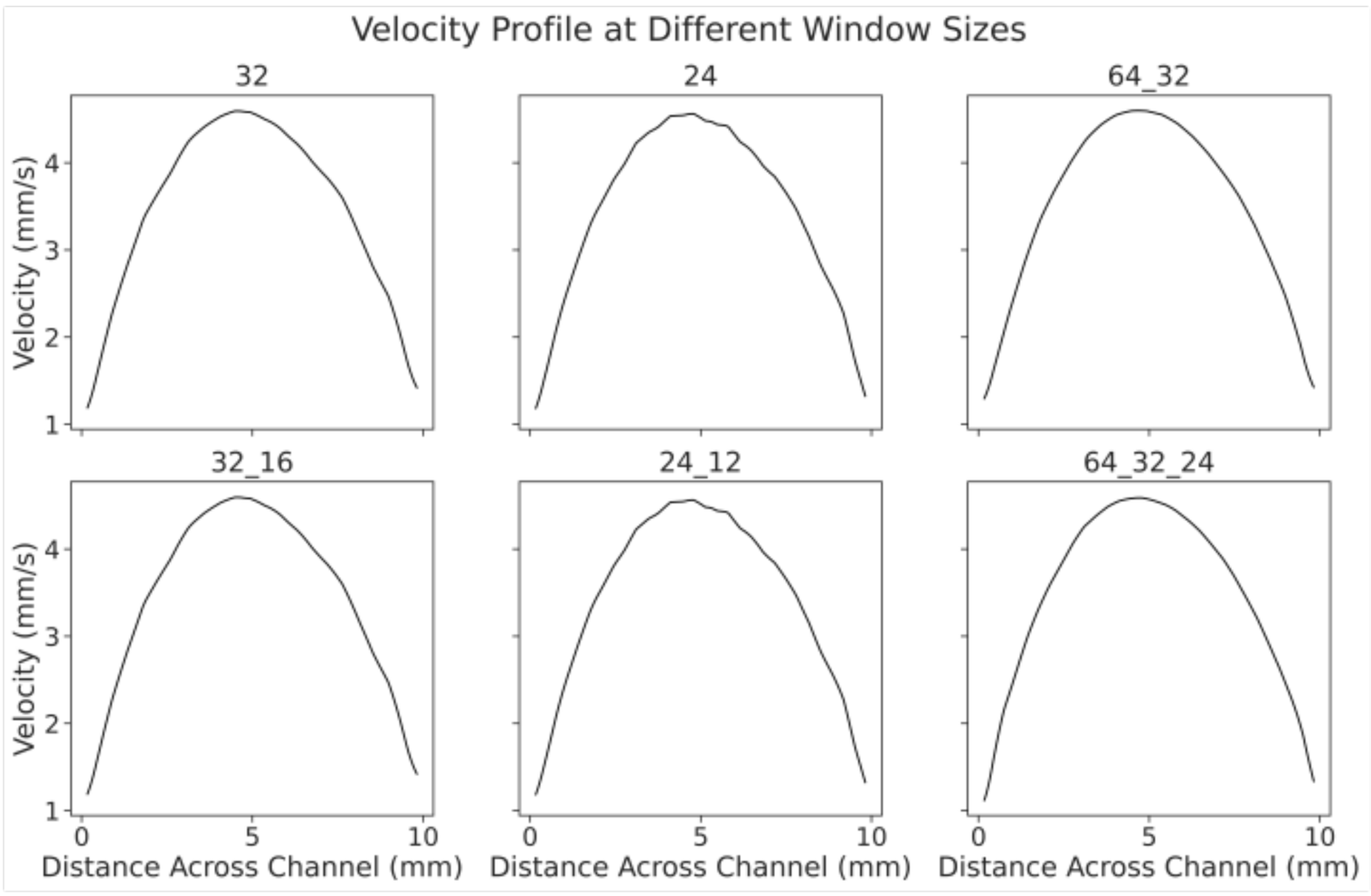

Figure 9: Velocity profile accross channel width

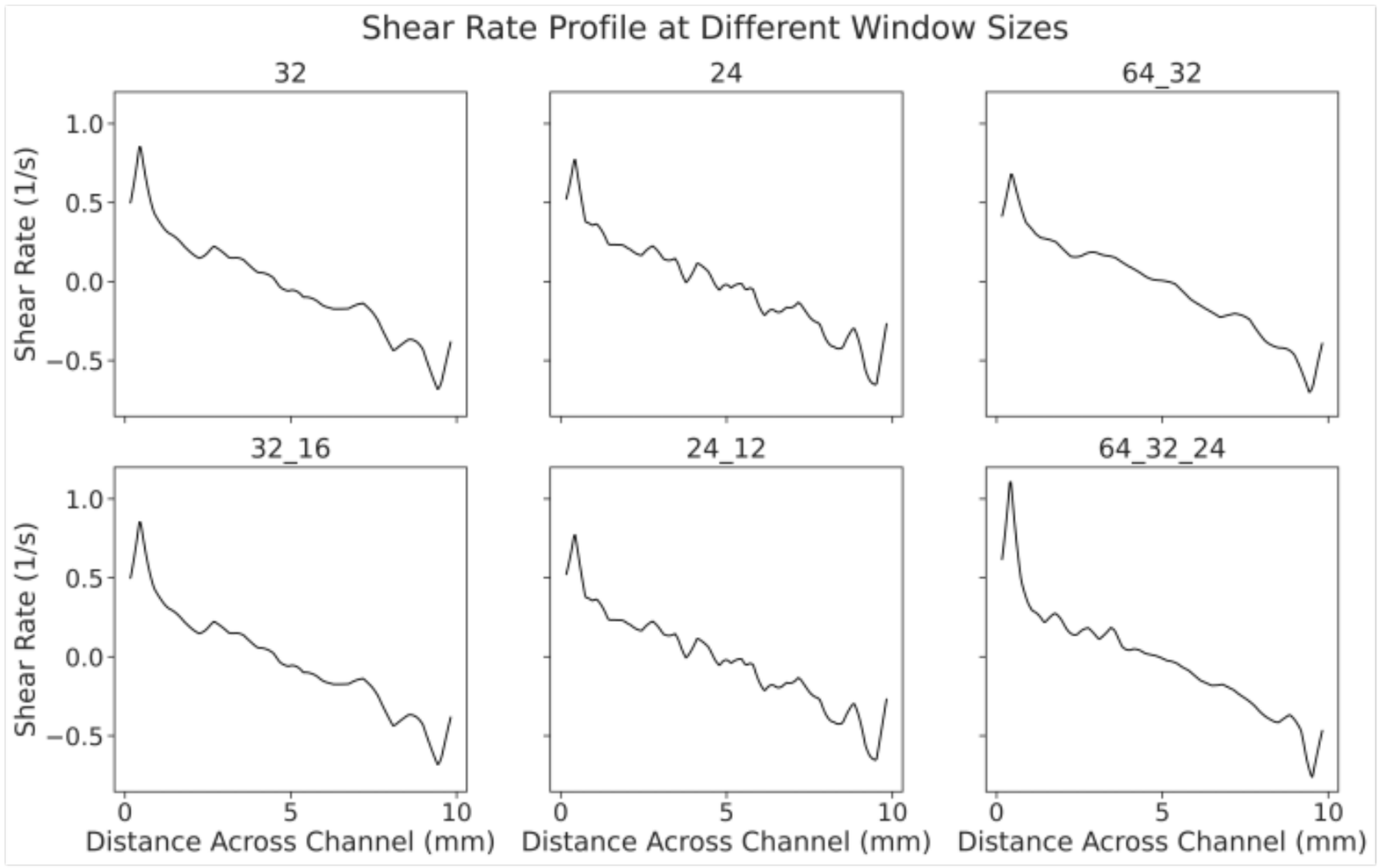

Figure 10: Shear rate profile accross channel width

for the high speed moving tracers at the center of the flow, but also the very slow moving tracers at the edges (boundary layer), where the high shear rate taxes place.

To get a sense of the magnitude of the effect of the afformentioned window size configurations, the shear rate was also plotted accross the channel width. The 64-32-24 pixel window configuration is undoubtedly the best configuration for my experiment as it is able to pertain the differences in velocity measurements. Looking at the bottom far right subplot, it can be seen that this configuration is able to account for the fast changing velocity values at the boundary layer (high value means higher derivative value). On the other hand, the rest of the configurations follow behind with the 24-12 pixel window configuration beting the worst of all, as the shear rate profiles are very sharp (unrealistic change in velocity change).

5 Conclusion

In this paper, a brief background and theory were given on PIV. In addition to that, a parametric study of different window size configuration was conducted to see it's affect on the accuracy of the PIV measurement. Six different configurations were tested, two of which were one-pass configurations (32 and 24 pixels), while the remaining four were multi-pass configurations (64-32, 32-16, 24-12 and 64-32-24 pixels). Out of all configurations, the 24 and 24-12 pixel window

performed the poorest. Both exhibited sharp velocity profiles and unrealistiv shear rate profiles. This is due to the fact that 24 pixels is a small window size for my setup. Most tracers were leaving the window between two instances. The 32 and 32-16 performed a lot better than the previous two configurations, but still had some jagged velocity profiles, as well as sharp edges with the shear rate profile. But the best configuration was the 64-32 and 64-32-24, with the three pass configuration performing a little better. Having three passes not only showed smooth velocity profiles, but also accounted for the high shearing at the boundary layer.

References

1. Hamdi, M., Havet, M., Rouaud, O. & Tarlet, D. Comparison of different tracers for PIV measurements in EHD airflow. *Experiments in Fluids* **55.** https://doi.org/10.1007%2Fs00348-014-1702-z (Mar. 2014).
2. Raffel, M., Willert, C., wereley steven, s. & Kompenhans, J. *Particle Image Velocimetry: A Practical Guide* ISBN: 9783540723073. https://books.google.com/books?id=WH5w2TvK2bQC (Springer Berlin Heidelberg, 2007).
3. Shavit, U., Lowe, R. J. & Steinbuck, J. V. Intensity Capping: a simple method to improve cross-correlation PIV results. *Experiments in Fluids* **42,** 225–240. https://doi.org/10.1007%2Fs00348-006-0233-7 (Dec. 2006).
4. Thielicke, W. *The flapping flight of birds: Analysis and application* PhD thesis (University of Groningen, 2014).